Supporting Information

Li et al. 10.1073/pnas.1320638111

SI Materials and Methods

Cell Culture. Melanoma cell lines WM793B, 1205Lu, WM115, and WM266-4 were provided by Meenhard Herlyn (Wistar Institute, Philadelphia, PA) and grown in the "2% tumor medium" containing 2% FBS and other components as previously described (1). Colon cancer cell lines KM12C and KM12SM and prostate cancer cell lines PC3M (also referred to as PC3) and PC3M-LN4 (referred to as LN4) were provided by Isaiah Fidler (MD Anderson Cancer Center, Houston, TX) (2, 3). Colon cancer cell lines SW480 and SW620 and prostate cancer cell lines DU145 and LNCaP were obtained from the American Type Culture Collection (ATCC). KM12C and KM12SM cells were grown in DMEM supplemented with 10% (vol/vol) FBS, sodium pyruvate, nonessential amino acids, L-glutamine, and vitamin solution. PC3, LN4, DU145, and LNCaP cells were cultured in RPMI supplemented with 10% FBS. SW480 and SW620 cells were grown in DMEM with 10% FBS. All cell lines were grown at 37 °C with humidified atmosphere and 5% CO_2.

shRNA Screens. We performed primary arrayed RNAi screens using a lentiviral library expressing ~2,100 shRNAs against ~440 human kinases on four pairs of cell lines. The first line of each pair was poorly metastatic and the other is highly metastatic: (*i*) PC3M and PC3M-LN4 prostate cancer (3); (*ii*) WM793B and 1205Lu melanoma (1); (*iii*) WM115 and WM266-4 melanoma (1); and (*iv*) KM12C and KM12SM colon cancer (2). The match between the PC3M cells and the ATCC PC3 cells and between the two cell lines in each pair was validated by DNA fingerprinting (data not shown).

Library glycerol stocks of human kinome shRNAs in LKO.1 vector were handled as recommended by The RNAi Consortium (TRC) (4). High-throughput, high-quality DNA preparation has been described (5), and DNA concentration was determined by using Hoechst dye (6). Preexperiments were performed for each cell line to determine its suitability for 384-well plate screening experiments, its optimal cell number per well, and shRNA lentiviral dose. Primary screens on the four pairs were done with the optimal viral dose for each pair (with and without puromycin selection, 1 μg/mL), except for the PC3/LN4 pair that were screened with two viral doses. Effects of each shRNA on cell survival and proliferation was determined 5 to 6 d after transduction by quantifying reduction of Alamar blue, a measure of mitochondrial fitness and a surrogate marker for cell number (6, 7). Measurements were then normalized to average of multiple scrambled negative control shRNAs as percentages of cell growth. The screens were reproducible with an average correlation coefficient of 0.85 among replicate screens of same cell lines (Fig. S1).

To identify kinase shRNAs that preferentially inhibited metastatic cells, we established the following criteria in the primary screens: (*i*) their shRNAs inhibited at least one metastatic cell line by greater than 50% relative to control shRNA, irrespective of survival or proliferation; (*ii*) their shRNAs inhibited metastatic cells at least 25% greater than in the parental poorly metastatic cells; and (*iii*) they had at least two independent shRNA sequences that scored in the screens. We then conducted a series of studies as secondary screens to identify kinases from this set with properties that might suggest a role in metastasis or tumor development. These tests included shRNA lentiviral titration experiments, preliminary genomic analysis for point mutations or amplifications in human cancers, and various cell-based assays related to metastasis. Criteria for selecting kinases from these secondary screens were shRNA silencing preferentially inhibited multiple metastatic cell lines, potential genetic alterations (i.e., mutation or amplification) in human cancers, or cDNA scored in one of our cell-based assays. Application of these criteria resulted in 38 kinases. Among them were eight kinases that have been previously established in cancer and metastasis, including KDR (8), FLT3 (9), NTRK1 (10), NTRK2 (11), AKT3 (12), PDK1 (13), CDK4 (14), and FYN (15). Identification of these eight kinases served as proof of principle for the screen and validated our approach. However, because our goal was to identify novel regulators, we chose to focus on the remaining 30 kinases that were less well established with regard to metastasis for in vivo validation (Fig. S2).

Orthotopic Prostate Cancer Xenograft. Cells transduced with pooled viruses for multiple kinase cDNAs or singular viruses for individual kinase cDNAs were selected with blasticidin (7.5 μg/mL). GFP was used as control. Two million cells in PBS solution were injected into the prostate gland of male ICR/SCID mice. The mice were killed 8 or 12 wk after injection to examine for tumor growth in prostates or in metastatic sites. All animal experiments were performed under protocols approved by The Institutional Animal Care and Use Committee (IACUC) of Boston Children's Hospital.

Inducible Expression of shRNAs in Vitro and in Vivo. The shRNA targeting sequences are CCTAAGGTTAAGTCGCCCTCG (scrambled control), GAGTTCAGTGTGCATAGGATT [G-protein–coupled receptor kinase 3 (GRK3) shRNA-1], CAGCCCTTTCAGACAACATAA (GRK3 shRNA-2), and AACACGTACAAAGTCATTTAT (GRK3 shRNA-3). Procedure of cloning GRK3 and scrambled shRNAs into Tet-On inducible shRNA vector was same as cloning shRNAs into pLKO.1 vector as recommended by TRC (4). LN4 cells carrying inducible shRNAs were established through transduction and G418 selection (0.4 mg/mL). shRNA expression was induced by adding doxycycline (0.8 μg/mL) into the media. Cells were lysed 72 h later for Western blotting (without overt cell death caused by GRK3 shRNA-1). LN4 cells carrying inducible scrambled control shRNA or inducible GRK3 shRNA-1 were injected into prostates of two cohorts of male ICR/SCID mice. Two weeks later, doxycycline was administrated i.p. daily for 4 wk before the mice were killed and the tumor tissues were weighed.

Microarray Analysis and Real-Time PCR for GRK3-Regulating Genes. Total RNA was extracted using Qiagen RNeasy plus kit with genomic DNA elimination. Replicate microarray experiments were done using Illumina Ref8-v3 BeadChips. The procedure and data analysis were completed according to the guidance of Qiagen and Illumina. Raw data were normalized by using an average normalization algorithm. Our microarray experiments were highly robust with correlation coefficients of 0.992 to 0.997 among replicates. The data have been deposited into the Gene Expression Omnibus database (accession no. GSE36022). Probe-based real-time PCR was done by using a Roche LightCycler 480 instrument with primers and probe combinations for each examined gene as recommended by Roche (www.roche-applied-science.com/sis/rtpcr/upl/ezhome.html).

Western Blot for GRK3, TSP-1, and Plasminogen Activator Inhibitor 2. Cells were harvested by mechanical scraping into 4 °C PBS solution, and cell pellets were obtained by removing PBS solution after centrifugation at 14,000 × *g* in a Microfuge device for 2 min. Cells were then lysed in 50 mM Tris·Cl (pH 7.4), 150 mM NaCl,

1% Nonidet P-40, 1 mM sodium orthovanadate, 5 mM NaF, 20 mM β-glycerophosphate, and complete protease inhibitor. Protein concentrations were determined by the BioRad protein assay. Fifteen to fifty micrograms of protein were loaded per well onto a 4% to 12% precast Bis-Tris gel. Protein extracts were electrophoresed and transferred to an Immobilon-P membrane. The membranes were blocked in 5% nonfat milk and incubated in primary antibody for TSP-1, GRK3, plasminogen activator inhibitor 2 (PAI-2), or β-actin. The membranes were then washed in TBS plus 0.1% Tween-20 and incubated with HRP-conjugated secondary antibody, followed by another wash. The membrane was then developed with ECL reagent and exposed on film.

Tumor Cell and Endothelial Cell Migration. Classic migration and invasion assays were performed using Corning Transwell Chambers and BD BioCoat-Matrigel Invasion Chambers, respectively, according to manufacturer guidance. Briefly, PC3-GFP and PC3-GRK3 cells were serum starved for 12 to 18 h. Fifty thousand PC3-GFP and PC3-GRK3 cells in serum-free RPMI media were seeded on the upper chambers of 24-well Transwell chambers or Invasion chambers with 8 μm pore size membrane. RPMI media containing 2.5% (vol/vol) FBS was added to the lower chambers and the upper/lower chambers were incubated for 24 h. The cells migrating or invading to the bottom side of the membrane were then stained with 2% crystal violet in ethanol for 1 h, washed with water, and counted in five random fields by using an Olympus microscope at a magnification of 10×.

For endothelial cell migration assay, 20,000 human lung microvascular endothelial cells (Lonza) were seeded in the upper chamber and 100,000 PC3-GFP, PC3-GRK3 cells in low serum media, or low serum media alone were placed in the lower chamber, at which time the upper chambers were placed into the wells and incubated with the lower chambers for 12 h. The procedure of staining and counting migrated endothelial cells is similar to that for migrated cancer cells described earlier.

Immunohistochemistry and Immunofluorescence Staining. ***Micrometastasis Detection in Xenograft Mouse Model.*** For detection of micrometastases in lungs and livers of mice orthotopically injected with PC3-GFP or PC3-GRK3 cells, standard sections (5 μm) of paraffin-embedded mouse lung and liver tissues were dewaxed with xylene/ethanol before antigen retrieval by Proteinase K for 5 min. Endogenous peroxidase activity was blocked. The slides were incubated with anti-human cytokeratin (Becton Dickinson) for 30 min at room temperature (RT) at a dilution of 1:10. Detection was done by using the EnVision HRP method (Dako), and the peroxidase was localized by the diaminobenzidine tetrachloride peroxidase reaction and counterstained with hematoxylin for 3 min.

CD34, Ki-67, and CD31 Staining for Angiogenesis in the Xenograft Mouse Model. Staining for microvessels and vascular proliferation was performed by dual immunohistochemistry (IHC) using a pan-endothelial marker CD34 rat anti-mouse antibody and Ki-67 rat anti-mouse antibody for endothelial cell proliferation (termed vascular proliferation). Sections were deparaffinized, rehydrated, and rinsed in distilled water. Heat-induced epitope retrieval was achieved by heating sections in target retrieval solution in a microwave oven for 20 min. Sections were allowed to cool at RT for 20 min and then further cooled under running water. After thorough rinsing in wash buffer (Dako), nonspecific staining was blocked by applying dual block (Dako) for 8 min. Further thorough rinsing in between all of the steps was done by incubating with buffer solution ×2 for 5 min in each rinse. Ki-67 antibody (diluted 1:50; Dako) was applied, followed by incubation with an alkaline phosphatase-conjugated secondary goat anti-rat antibody (diluted 1:100; Santa Cruz Biotechnology). Ferangi Blue Chromogen Kit (Biocare Medical) was applied for 20 min to visualize Ki-67. After rinsing, sections were incubated with denaturing solution (Biocare Medical) applied for 5 min. This was followed by incubating with CD34 rat anti-mouse antibody (diluted 1:50; Abcam). Then, HRP-conjugated secondary goat anti-rat antibody (diluted 1:50; Santa Cruz Biotechnology) was applied for 30 min. Finally, incubation with AEC+ substrate chromogen (Dako) for 20 min was used to visualize CD34. No contrast staining was applied, and final rinsing was done in distilled water. Then sections were mounted with aqueous solution (Dako).

For CD31 immunofluorescence staining, after deparaffinization and rehydration, the sections were treated with Target Retrieval Solution (DakoCytomation). These sections were incubated with blocking solution for 1 h followed by overnight incubation with primary antibody against CD31 (1:100 dilution; BD Pharmingen) in PBS solution containing 1% BSA at 4 °C. Slides were washed in PBS solution and then incubated with Alexa 594 (1:500 dilution; Invitrogen)-conjugated anti-rat IgG and DAPI for nuclear staining for 1 h at RT. The stained tissues were examined by using a fluorescence microscope (Axiovision Z1; Carl Zeiss). Control slides were processed similarly except for the omission of primary antibodies (data not shown).

Microvessel Density in the Xenograft Mouse Model. The average microvessel density (MVD) in tumor tissue was assessed in accordance with the Weidner approach, with minor modifications (16). MVD was examined in all consecutive high-power fields (magnification of 250×; field size 0.45 mm^2) that were available for a given case. The total number of high-power fields assessed ranged from 2 to 10. All positively stained vessels were counted including vessels without microlumina according to previous studies (16), and clusters of endothelial cells clearly separate from adjacent microvessels were also counted. Statistical analysis was performed by using SPSS Statistics version 19 (SPSS/IBM). MVD was compared between GRK3 and GFP tumors by using a Mann–Whitney U test. A P value ≤ 0.05 was considered significant.

GRK3 IHC Staining on Human Prostate Tumor Tissue Microarray. A consecutive series of 104 men (median, 62.0 y) treated by radical prostatectomy for clinically localized cancer (during the time period of 1988–1994). In addition, 33 castration-resistant prostate cancers (median, 77.3 y), 13 skeletal metastases, 33 soft-tissue metastases (28 from lymph nodes), and 41 cases of benign prostatic hyperplasia were included. Briefly, three tissue cores (diameter, 0.6–1.0 mm) were obtained from representative areas of highest tumor grade. Tissue microarray sections were used for all tissue subgroups except regular sections of the 13 skeletal metastases. Staining with anti-GRK3 was performed on formalin-fixed and paraffin-embedded tissues by using 5-μm sections. After boiling under pressure in TRS6 buffer (pH 6.0) for 15 min at 350 W, sections were incubated for 2 h at RT with GRK3 antibodies [HPA000804 (Sigma) and EPR2041 (Epitomics)] diluted 1:50, and stained with HRP EnVision rabbit (Dako) for 30 min at RT. The peroxidase was localized by the diaminobenzidine tetrachloride peroxidase reaction and counterstained with Mayer hematoxylin. Negative controls were obtained by omitting the primary antibody. A staining index (values 0–9) was calculated as a product of staining intensity (values 0–3) and the proportion of positive tumor cells (0%, score of 0; <10%, score of 1; 10–50%, score of 2; and >50%, score of 3). Associations between variables were assessed by Pearson χ^2 and Kruskal–Wallis tests. The SPSS statistical package, version 19.0 (SPSS), was used.

Glomeruloid Microvascular Proliferation. Glomeruloid microvascular proliferation (GMP), or vascular nests, is considered a marker of VEGF-A driven angiogenesis. GMPs were stained and recorded as previously reported (17). Briefly, from 104 patients with localized prostate cancer, 5-μm sections of formalin-fixed and paraffin-embedded archival tissue were used. Standard slides were stained with factor VIII antibody, and GMPs were recorded as being absent or present.

1. Satyamoorthy K, et al. (1997) Melanoma cell lines from different stages of progression and their biological and molecular analyses. *Melanoma Res* 7(suppl 2):S35–S42.
2. Morikawa K, et al. (1988) Influence of organ environment on the growth, selection, and metastasis of human colon carcinoma cells in nude mice. *Cancer Res* 48(23): 6863–6871.
3. Pettaway CA, et al. (1996) Selection of highly metastatic variants of different human prostatic carcinomas using orthotopic implantation in nude mice. *Clin Cancer Res* 2(9): 1627–1636.
4. Moffat J, et al. (2006) A lentiviral RNAi library for human and mouse genes applied to an arrayed viral high-content screen. *Cell* 124(6):1283–1298.
5. Pearlberg J, et al. (2005) Screens using RNAi and cDNA expression as surrogates for genetics in mammalian tissue culture cells. *Cold Spring Harb Symp Quant Biol* 70: 449–459.
6. Nakayama GR, Caton MC, Nova MP, Parandoosh Z (1997) Assessment of the Alamar Blue assay for cellular growth and viability in vitro. *J Immunol Methods* 204(2): 205–208.
7. O'Brien J, Wilson I, Orton T, Pognan F (2000) Investigation of the Alamar Blue (resazurin) fluorescent dye for the assessment of mammalian cell cytotoxicity. *Eur J Biochem* 267(17):5421–5426.
8. Zhang H, Wu J, Meng L, Shou CC (2002) Expression of vascular endothelial growth factor and its receptors KDR and Flt-1 in gastric cancer cells. *World J Gastroenterol* 8(6):994–998.
9. Timeus F, et al. (2001) Flt-3 and its ligand are expressed in neural crest-derived tumors and promote survival and proliferation of their cell lines. *Lab Invest* 81(7):1025–1037.
10. Teixeira MR (2006) Recurrent fusion oncogenes in carcinomas. *Crit Rev Oncog* 12(3-4): 257–271.
11. Thiele CJ, Li Z, McKee AE (2009) On Trk—the TrkB signal transduction pathway is an increasingly important target in cancer biology. *Clin Cancer Res* 15(19):5962–5967.
12. Dillon RL, Muller WJ (2010) Distinct biological roles for the akt family in mammary tumor progression. *Cancer Res* 70(11):4260–4264.
13. Raimondi C, Falasca M (2011) Targeting PDK1 in cancer. *Curr Med Chem* 18(18): 2763–2769.
14. Blain SW (2008) Switching cyclin D-Cdk4 kinase activity on and off. *Cell Cycle* 7(7): 892–898.
15. Saito YD, Jensen AR, Salgia R, Posadas EM (2010) Fyn: A novel molecular target in cancer. *Cancer* 116(7):1629–1637.
16. Weidner N, Semple JP, Welch WR, Folkman J (1991) Tumor angiogenesis and metastasis—correlation in invasive breast carcinoma. *N Engl J Med* 324(1):1–8.
17. Straume O, et al. (2002) Prognostic importance of glomeruloid microvascular proliferation indicates an aggressive angiogenic phenotype in human cancers. *Cancer Res* 62(23):6808–6811.

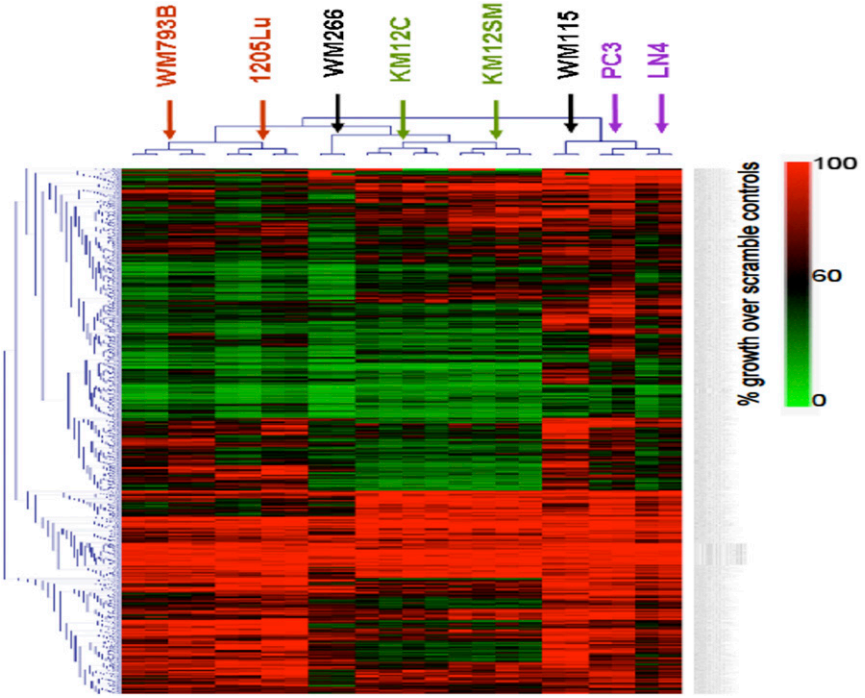

Fig. S1. Paired human poorly and highly metastatic cell lines responded similarly to expression of shRNAs again human kinases. Each of the eight cell lines on the *x* axis was screened with a human kinase shRNA library (*y* axis) multiple times through transduction in arrayed format. Percentage of cell growth for each shRNA was normalized to scrambled control shRNA. Shown is the heat map from unsupervised hierarchical clustering analysis using percentage of cell growth. Green color in the heat map indicates low cell growth (good inhibition) and red indicates high cell growth (poor inhibition). Colored arrows on the *x* axis indicate paired cell lines. Replicate screens on the same cell lines are clustered together tightly. The two paired lines are more similar to each another in three pairs. The pair in black did not cluster together (WM115 and WM266). It is the only pair in which the metastatic line was derived from a metastatic lesion of the same patient from whom the poorly metastatic line was obtained. Meanwhile, the metastatic lines of the other three pairs were derived from metastatic tumors through several rounds of in vivo selection in mice using the parental poorly metastatic lines as the source of the initial cells. The Alamar blue assays were typically done at 5 to 6 d after transduction, at which point the scrambled control cells had reached confluence; therefore, the screens were not optimized to identify shRNAs that promote better proliferation than the scramble control shRNA. The assay did not distinguish effects on cell survival or proliferation.

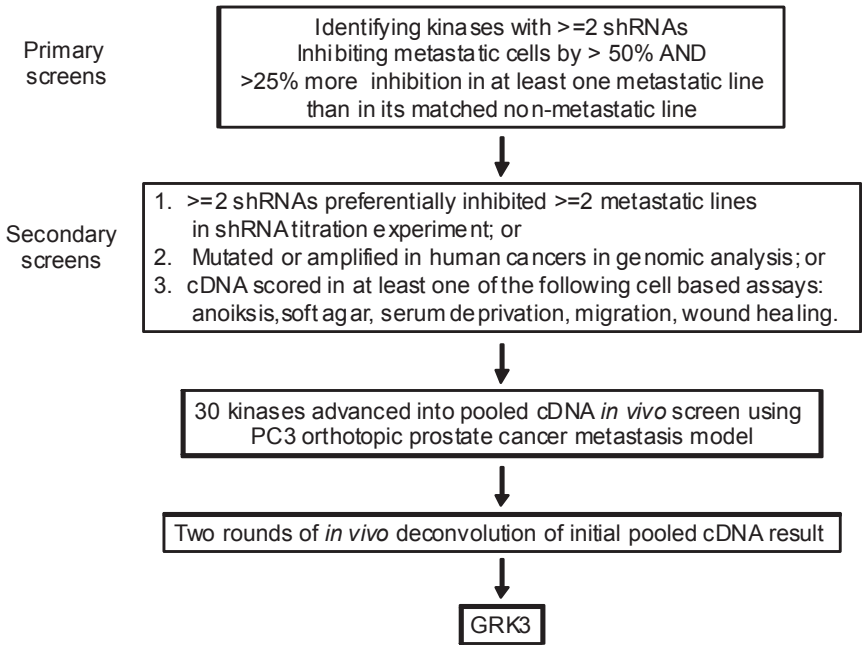

Fig. S2. Hit identification and prioritization process. Human kinases scored from primary shRNA screens as essential for survival and proliferation of metastatic cells were further prioritized through shRNA titration experiments, genetic analysis, or cell-based assays. From these studies, 30 kinases were selected for a pooled in vivo study by using PC3 orthotopic prostate cancer metastasis xenograft model. Upon two rounds of deconvolution in mice, GRK3 was discovered as a kinase that could promote primary tumor growth and metastasis when overexpressed in poorly metastatic PC3 cells.

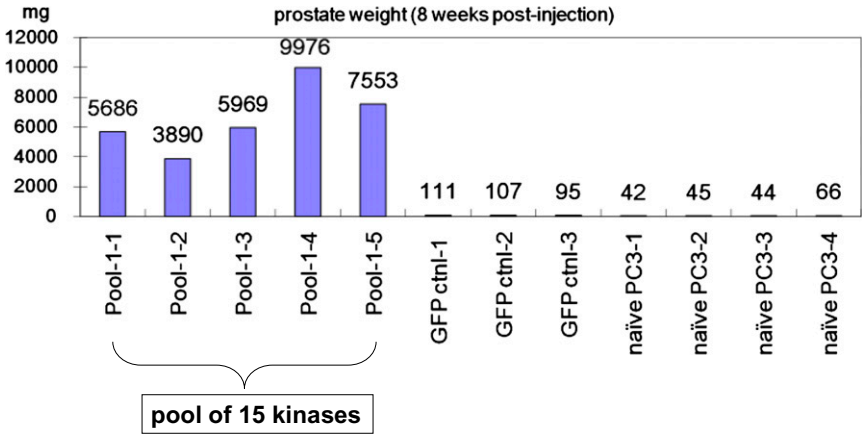

Fig. S3. Orthotopic tumor growth in prostate from first-round cDNA in vivo experiment with 15 kinases in one pool (pool 1). Naïve PC3 cells or PC3 cells infected with GFP virus or pooled viruses for 15 essential kinases were injected into prostates of male SCID mice. Mice were killed 8 wk later, and sizes and weights of their prostates were measured. Shown on the *y* axis are weights of prostate in milligrams.

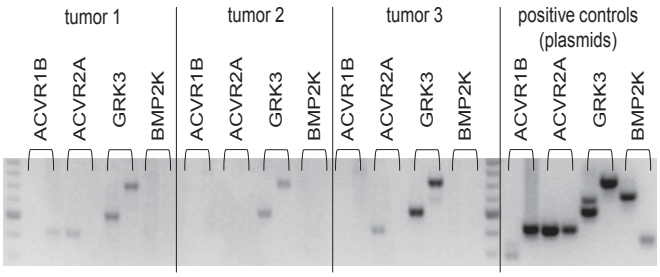

Fig. S4. Genomic PCR to specifically detect exogenous kinase cDNAs in prostate tumors from second-round in vivo cDNA experiment with four kinases in one subpool. The 15 kinases in pool 1 from the first round in vivo experiment were randomly divided into four subpools. All four subpools were tested in a second round, in which one subpool generated considerably larger primary tumors. Genomic DNA from the resultant prostate tumors of this subpool were extracted and screened via PCR using primers that specifically detected the four exogenous kinase cDNAs in this subpool. Retroviral vectors carrying kinase cDNAs were used as positive controls in PCR. Shown are PCR products at expected sizes from two sets of primers for each kinase in three tumors from this four-kinase subpool that contained ACVR1B, ACVR2A, BMP2K, and GRK3. GRK3 was the kinase that consistently dominated in these tumors. The other three tumors in this subpool showed a similar pattern (data not shown).

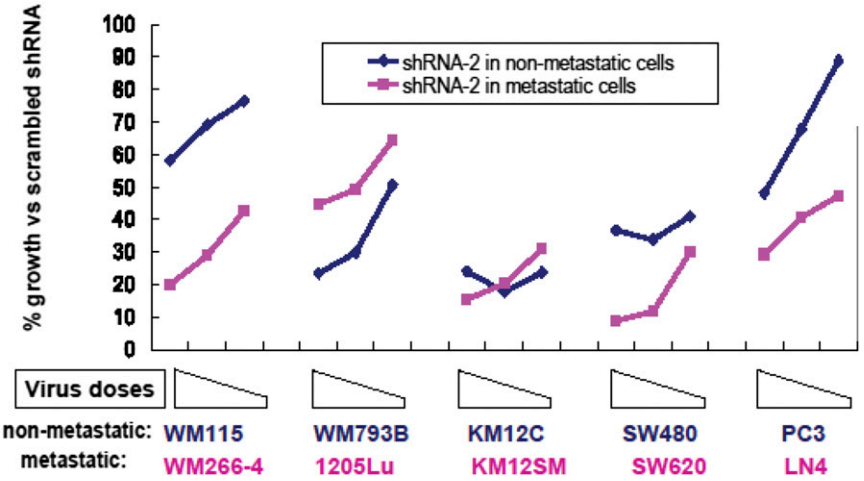

Fig. S5. GRK3 shRNA-2 preferentially inhibits the growth of metastatic cells in culture. The *x* axis denotes three doses of shRNA viruses used to infect five pairs of poorly metastatic cell lines (blue) and metastatic lines (pink). The *y* axis denotes percentage of cell growth normalized to scrambled control shRNA at each titration for each cell line. Three virus doses were used with twofold decrements from left to right. In the absence of puromycin selection, the effects were solely a result of the expression of shRNA. As virus doses decreases, the percentage of cell growth increases as expected.

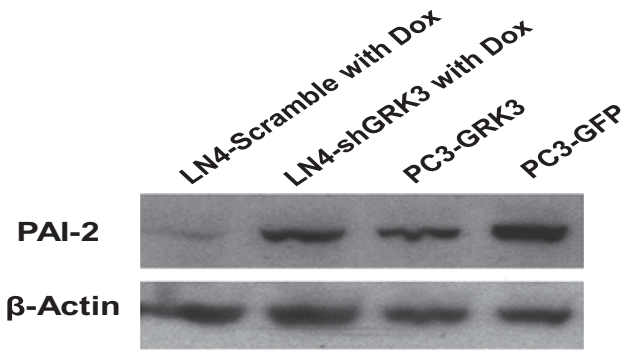

Fig. S6. Expression of PAI-2 in PC3 and LN4 cells upon modulation of GRK3 expression. GRK3 was up-regulated by cDNA transduction in PC3 cells or down-regulated by doxycycline-induced shRNA expression in LN4 cells. Protein level of PAI-2 was then examined through Western blotting.

Table S1. Thirteen genes that are implicated in wound healing and also regulated by GRK3

Gene ID	Name	Symbol	GRK3/GFP fold
3553	interleukin 1, β	IL1B	0.37
5055	Plasminogen activator inhibitor-2	PAI-2	0.46
3569	interleukin 6 (IFN, β2)	IL6	0.51
7057	thrombospondin 1	TSP-1	0.53
316	aldehyde oxidase 1	AOX1	0.59
7980	tissue factor pathway inhibitor 2	TFPI2	0.62
1316	Kruppel-like factor 6	KLF6	0.63
1839	heparin-binding EGF-like growth factor	HBEGF	0.66
2244	fibrinogen β-chain	FGB	1.52
64332	nuclear factor of κ light polypeptide gene enhancer in B-cells inhibitor, ζ	NFKBIZ	1.62
6279	S100 calcium binding protein A8	S100A8	1.68
1490	connective tissue growth factor	CTGF	1.70
9060	3′-phosphoadenosine 5′-phosphosulfate synthase 2	PAPSS2	1.86